

Computer vision detection of peel defects in citrus by means of a region oriented segmentation algorithm

J. Blasco^{a,*}, N. Aleixos^b, E. Moltó^a

^a Centro de AgroIngeniería, Instituto Valenciano de Investigaciones Agrarias (IVIA), Carretera Moncada-Náquera km 5, 46113 Moncada (Valencia), Spain

^b Departamento de Ingeniería Mecánica y de Construcción, Universitat Jaume I de Castelló (UJI), Campus Riu Sec, 12071 Castelló, Spain

Received 5 October 2006; received in revised form 30 November 2006; accepted 2 December 2006

Available online 22 December 2006

Abstract

Due to the high sorting speed required during fruit inspection and classification in packing lines, most of the current automatic systems, based on machine vision, normally employ supervised techniques oriented towards individual pixels to segment the images of the fruits. These techniques require previous training given by experts in order to classify the colour of each pixel as belonging to any of the regions of interest and frequent training sessions during normal operation throughout the season to adapt the system to the great colour variability present in biological products like fruits. In region-oriented segmentation algorithms, however, the contrast between different areas in the image becomes more important than the individual pixel colour, thus solving the problem related to the variability of the natural colour of fruits. This work proposes a region-oriented segmentation algorithm for detecting the most common peel defects of citrus fruits. Focused on the detection of the regions of interest consisting of the sound peel, the stem and the defects, this method is an original contribution that allows successful segmentation of smaller defects, such as scale. The algorithm was tested on images of different varieties of oranges and mandarins presenting defects, without any further training being given between inspections of different batches, even species, of citrus fruits. Assuming that the most surface of the fruit corresponds to sound peel, the proposed algorithm was able to correctly detect 95% of the defects under study.

© 2006 Elsevier Ltd. All rights reserved.

Keywords: Defect detection; Machine vision; Image segmentation; Fruit quality inspection; Citrus fruits; Mandarins; Oranges

1. Introduction

For a long time, the agro-industry has attempted to automate fruit selection in order to decrease production costs and increase the quality of the production. In the packing lines, where most external quality attributes are currently inspected visually, machine vision provides a means of performing this task automatically. Current commercial systems are capable of calculating parameters such as size (Brodie, Hansen, & Reid, 1994), colour, shape or ripeness (Díaz, Faus, Blasco, Blasco, & Moltó, 2000; Hahn, 2002). The most advanced machines are also capable of detecting blemishes (Aleixos, Blasco, Navarrón, &

Moltó, 2002; Leemans & Destain, 2004), one of the most influential factors in the commercial quality of fruit, or even predict some internal features, as the sugar content (Steinmetz, Roger, Moltó, & Blasco, 1999).

In digital image processing, the success of the algorithms that perform the image analysis is largely dependent on the segmentation procedure, defined as the process used to subdivide the image into regions or objects of interest (Gonzalez & Woods, 2002). There are many techniques to segment images, including neural networks (Meuleman & Van Kaam, 2001; Díaz et al., 2004; Moshou, Bravo, West, McCartney, & Ramon, 2004; Kiliç, Hakki-Boyaci, Köksel, & Küsmenoğlu, 2007), *k*-means (Lucchese & Mitra, 1999), detection of pixels, detection of regions (Fu & Mui, 1981; Sun & Du, 2004), vector quantisation (Hofmann & Buhmann, 1998), vector support machines

* Corresponding author. Tel.: +34 963424000; fax: +34 963424001.

E-mail address: jblasco@ivia.es (J. Blasco).

(Du & Sun, 2005) and so forth. The selection of a particular method can depend on restrictions imposed by the problem at hand. This is the case of the segmentation algorithms commonly implemented in the automatic systems for on-line fruit grading, where the high speed required by these systems, obligate the segmentation procedure to be performed in a very short time (Aleixos, Blasco, & Moltó, 1999).

In pixel-oriented techniques, the aim is to classify each pixel as belonging to a particular region of interest. The colour of each individual pixel, expressed as coordinates in a three-dimensional space, is then used as the only feature to segment the image. Consequently, these systems must learn how to relate the colour of the pixels with the regions, thus making it a supervised method. This learning task, called training, is normally performed off-line by means of experts who acquire images, presumably containing the variability of the different regions, and manually assign the colour of the pixels to the predefined regions (Moltó, Aleixos, Blasco, & Navarrón, 2000). The information that describes the correspondence between the possible colours of the pixels and the regions is stored in the computer and used during on-line operation.

Techniques based on statistics, such as Bayesian methods, can facilitate this process (Marchant & Onyango, 2003), but still require the participation of an expert. In these cases, the expert selects only a few representative pixels of the colour of each region and calculates the probability of the rest of the possible colours' belonging to each region. Using these techniques, the systems need a shorter time to be trained but, because they are still oriented towards individual pixels, they continue to have the problems related with the variations in colour.

The quick processing speed of these methods allow their implementation in processes that require fast working speed, such as the on-line inspection of agricultural produce, but they are very sensitive to changes in the lighting conditions or in the colour of the fruits, which can vary significantly throughout the season. Even in fruits from the same batch, the peel and defects can present different colours, shapes, sizes and textures. Situations where the colour of a particular defect in one fruit matches the colour of the sound skin of other fruit are also common. A system based on the colour of individual pixels needs to be frequently adapted to meet these changes. For this reason, several different trainings are required during normal operation throughout the season.

In contrast, region-oriented methods analyse information about areas of the image before to classify the pixels in regions of interest. These methods use features contained in these areas, such as colour changes (Albiol, Torres, & Delp, 2001), boundaries (Martínez-Usó, Pla, & García, 2003), texture (Brox, Rousson, Deriche, & Weickert, 2003), regions (Bhalerao & Wilson, 2001), and so forth. Since the information used to classify one pixel is obtained from their surrounding area, these methods are robust

against colour variations and normally they do not need any training during the season.

Systems developed using unsupervised segmentation methods do not need any previous training because they are programmed to extract the information from the images. Generally, fruit images acquired by the automatic inspection systems have common particularities such as a homogeneous well-defined background, a homogeneous regular area corresponding to the sound skin and the more textured regions of the stem, calyx or defects that can be confused (Unay & Gosselin, 2007). This previous knowledge of the scenes facilitates the development of unsupervised algorithms to solve this particular problem (Noordam, Van Den Broek, & Buydens, 2003).

This work proposes an unsupervised region-growing algorithm to segment images of citrus fruits and automatically detect the most common external defects. The algorithm proposed uses colour to segment images of different varieties of oranges and mandarins without any previous training and without particular changes or adjustments for each kind of fruit. A new contribution has been made to the region-growing algorithm that allows segmentation of smaller defects, such as scale. Further morphological operations in the segmented image, including the estimation of the area, size or perimeter, can improve the detection of defects (Blasco, Aleixos, & Moltó, 2003), or reduce the number of false detections, which is not the aim of this work.

2. Objective

The objective of this work is to develop an algorithm to avoid the previous training needed by the fruit inspection image processing techniques commonly employed in the industry. To achieve this objective, an unsupervised algorithm adapted to the particular case of fruit inspection was developed. Being region-oriented, the contrast between different objects of interest in the image becomes more important than the individual pixel colour, thus avoiding the problems related with the lighting conditions and variations in the colour of the fruit.

3. Materials and methods

The sample of fruit, consisting of 356 oranges and 279 mandarins (635 fruits) belonging to different varieties, was provided by experts from a sorting machine manufacturing company. The algorithm was tested using images from all individual fruits, in which a total number of 2132 individual surface blemishes and 162 stems were visible. In the images, a particular fruit could contain no defects, or one or more blemishes corresponding to one defect (i.e., each of spots of phytotoxicity due to chemical product drops were considered as a different blemish). Following the recommendations of a producer company, the defects and diseases studied in the fruit were: medfly egg deposition, green mould caused by *Penicillium digitatum*,

oleocellosis (rind oil spot), scale, scarring, thrips scarring, chilling injury, stem injury, sooty mould, anthracnose and phytotoxicity. The fruits were randomly chosen in different moments of the season (corresponding with the different harvesting time of each variety) and the number of fruits of each defect was related with the frequency of apparition in a commercial packing line. Fig. 1 shows samples of the different defects studied. The distribution of them in the images of the different varieties of citrus fruit analysed is detailed in Table 1.

An inspection chamber was built for this specific purpose and mounted over a commercial conveyor, like those used to transport fruit in the on-line fruit inspection machines. The camera and the lighting system were placed inside this inspection chamber. The CCD (charge-coupled device) camera (Sony XC-003P), placed 400 mm above the scene, provided the video in the RGB (red, green, blue) coordinates. The illumination system consisted of eight fluorescent tubes (25 W each). Polarised filters were placed in front of the fluorescent tubes and coupled to the camera

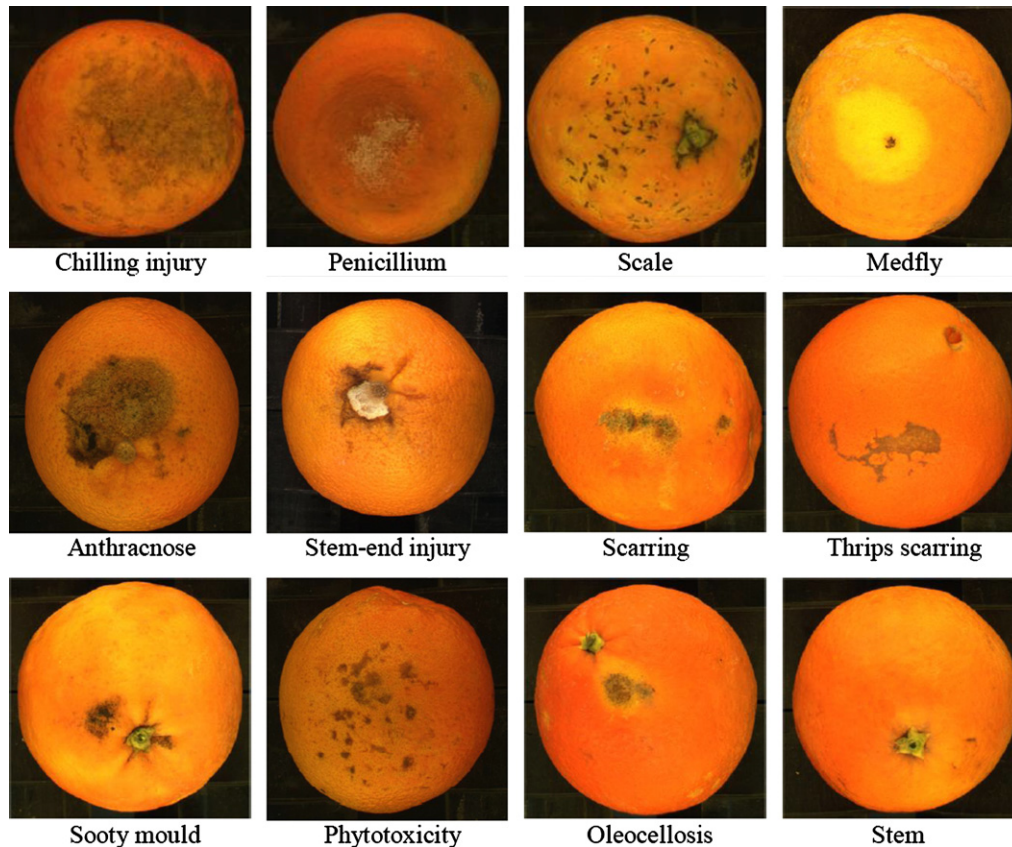


Fig. 1. Sample images of the defects that were studied.

Table 1

Distribution of the defects and stem in the images of the fruit used for the experiments

	Navelina Valencia		Marisol	Clemenules	Fortune	Total defects
Medfly	27	0	9	5	0	41
Sooty mould	29	17	15	11	0	72
Thrips scarring	357	88	95	77	119	736
Scarring	98	48	30	18	56	250
Oleocellosis	32	17	18	16	16	99
Scale	98	71	116	46	62	393
Green mould	16	12	11	7	11	57
Phytotoxicity	92	65	0	0	56	213
Chilling injury	97	81	0	0	0	178
Stem-end injury	0	9	11	11	8	39
Anthracnose	14	13	14	0	13	54
Stem	40	32	33	24	33	162
Total defects/variety	900	453	352	215	374	2294

lens to reduce the bright spots of the scene by means of cross polarisation. All the elements (showed in Fig. 2) were mounted inside an inspection chamber. The images, with a size of 768×576 pixels and a resolution of 0.17 mm/pixel, were acquired using the camera and a frame grabber (Matrox Meteor II) plugged into a personal computer. The images were acquired by placing the fruit inside the inspection chamber, manually orienting the side of the fruit that contained the defects towards the camera. Each image was saved in TIFF (tagged image file format) with a name related to the variety, type and number of the defects.

3.1. Description of the algorithm

The objective of this algorithm is to segment the regions in the image that represent the sound peel, the defects and the stem. In the first step, the segmentation algorithm has to set up the seeds (starting points) of each possible region. This step starts with the detection of the regions in the image with a homogeneous colour (large areas with soft texture and smooth colour changes). Then, a seed is created in the middle of each homogeneous region that grows by iteratively adding the neighbouring pixels that accomplish a criterion of colour homogeneity. Once all of the pixels in the image have been assigned to one of the regions, the regions obtained are merged in accordance with a convergence criterion based on colour and neighbourhood. Finally, the largest region is assumed to be sound peel and the rest of the regions are considered as blemishes.

3.1.1. Pre-processing

The success of the image segmentation procedure largely depends on the correct selection of the seeds. The histogram of the images clearly showed a peak in the lower val-

ues corresponding to the background, since it was a uniform black colour that contrasted against the orange colour of the fruits. An algorithm for automatically determining this peak and removing the information about the background from the image was programmed.

The roughness of orange skin produces a texture that makes the segmentation method unable to find good seeds to start the process, since it prevents the existence of well-defined regions. For this reason, it is important to implement a first step for smoothing the image and removing the noise, while preserving the information about colour and the details of the objects. The algorithm used for the smoothing was based on 'peer group filtering', which consisted in replacing the colour of each pixel in the image with the average colour of the neighbouring pixels with a similar colour (Kenney, Deng, Manjunath, & Hewer, 2001).

The region-growing algorithm developed in this study can work with full colour images. However, in images with more than 256 colours, the computational cost is too high, needing the system more than 30 min to process each image. It was necessary to make a reduction from the 2^{24} colours of the original images to an optimum number of colours. The human eye perceives colour changes better in uniform regions than in those where details are appreciated (Chadda, Tan, & Meng, 1994). To reduce the colour depth of the images without affecting their quality, the homogeneity of the image was considered in such a way that most of reduction was performed in the more homogeneous areas, while in detailed regions, such a stem or defects, the colour reduction was smaller. The algorithm designed to carry out this colour reduction was an adaptation of the GLA (Generalised Lloyd Algorithm) described by Lloyd (1982), which is based on the human perception of colours.

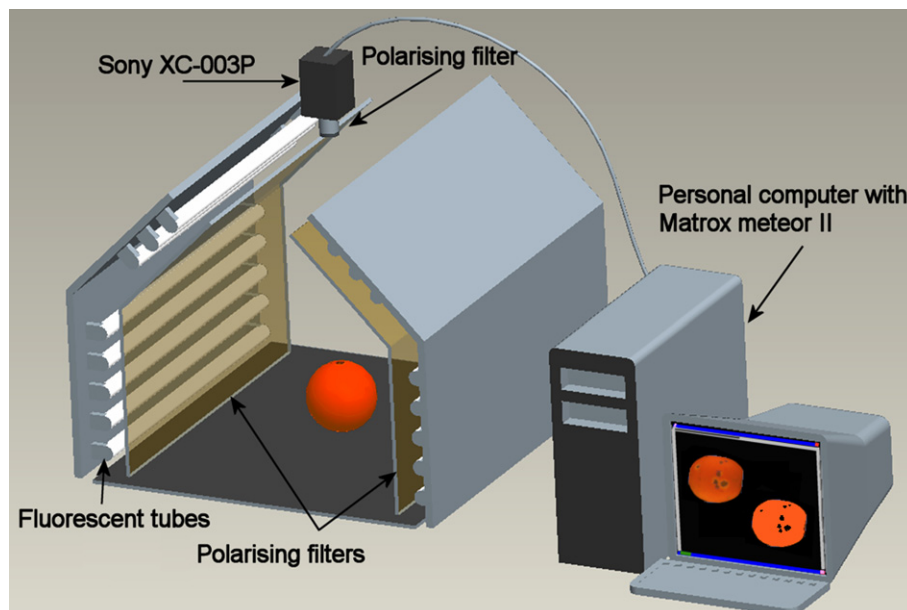


Fig. 2. Scheme of the acquisition system.

A preliminary test was conducted by reducing the number of different colours in the images to 8, 12, 16, 20, 32, 64 and 256 colours. It consisted in processing the same images of fruits (five random images of each variety) using the algorithm developed and counting the number of errors in the detection of the defects. Similar detection results were obtained in preliminary tests in images with 32, 64 and 256 colours, while with the use of fewer colours, some defects took on the same colour as that of the sound peel and thus, the number of false detections increased. The tests consisted in segmenting three images of fruits containing each different defect, using different reduction of colours and comparing the detection results with the visual inspection of the fruit. With a high number of colours, the images were excessively divided into regions, so the performance of the algorithm decreased. Since in images of 32 colours the computational cost is lower than using 64 or 256 colours, the optimum number of colours was fixed as being 32. Fig. 3 shows the image of an orange reduced to 32 colours using this method (left) and using a conventional colour reduction method based on the reduction of bit depth (right).

3.1.2. Seed selection

This is the initial step of the region-growing algorithm. The seed selection process was essentially based on the algorithm called JSEG, described in Deng, Manjunath, and Shin (1999), with some modifications (described later) so as to adapt and optimise the algorithm for the segmentation of citrus fruit images. The starting point of this algorithm was to determine seeds that properly represented regions of interest in the image. The initial set of seeds was located in the most homogeneous areas of the image; consequently, a homogeneity value was obtained for each pixel by analysing the local neighbourhood window of each pixel. Large neighbourhood windows are useful for detecting texture boundaries, so they are more appropriate for images with large regions, while small-sized ones are effective for detecting colour edges and small regions (Jing, Li, Zhang, & Zhang, 2003). The original algorithm is intended for segmenting general purpose images and uses circular neighbourhood windows from 9×9 to 65×65 pixels.

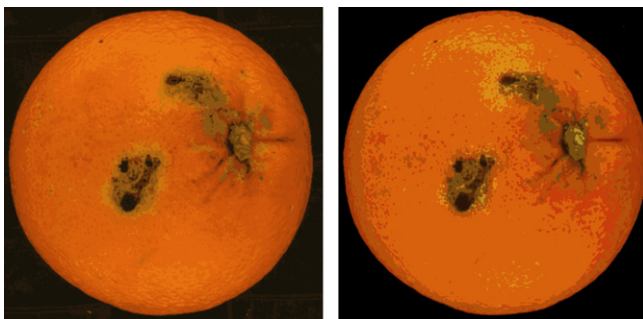


Fig. 3. Reduction to 32 colours performed with previous smoothing and the perceptual method (left) and by eliminating the less significant bits without previous smoothing (right).

However, the images of citrus fruits with skin defects have particular known features that are important to have in account to optimise the performance of the algorithm. In these images, there are no large variations in the texture of the sound peel but sharp changes between the peel and the defects are observed and there are present small defects, such as scale, that have to be analysed using smaller neighbourhood windows. It was decided to use a fixed square neighbourhood window of 3×3 pixels. Using larger neighbourhood windows, as 5×5 pixels, the success segmenting scale defects was 0%.

The values of the pixels corresponding to the homogeneity of their vicinity were normalised between 0 and 255. Those pixels located in the most homogeneous areas took the lowest values while the pixels in more detailed areas, such as boundaries, had the highest values. Then these values were used to establish a homogeneity threshold following Eq. (1)

$$T = \mu + \alpha\sigma \quad (1)$$

where μ was the average of the homogeneity values and σ was the standard deviation. After several tests, the constant α was assigned a value of 0.6.

The pixels with a value below the threshold were considered as potentially belonging to an initial seed. Finally, candidate pixels were grouped to form 4-connected clusters, and those with more than 32 pixels (approximately 1 mm^2) were considered as seeds. As an example, Fig. 4 shows a colour image and a new image showing the homogeneity values for each pixel. The boundary pixels are represented in white, while the pixels in the middle of large homogeneous areas are in shown in a dark colour.

3.1.3. Region-growing iteration

Region-growing was an iterative process that started with the original set of seeds. In each iteration the following tasks were performed:

- (a) the threshold T was recalculated by means of Eq. (1), using the average μ and standard deviation σ of those pixels that had still not been assigned to any seed.

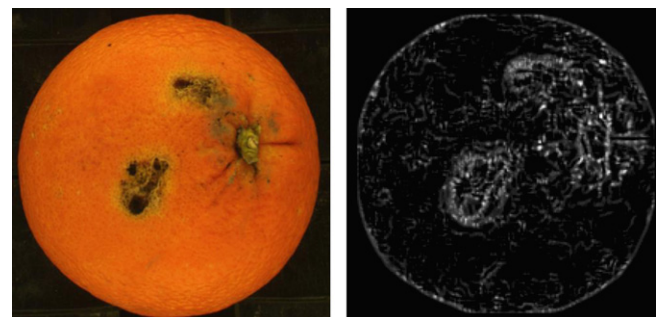


Fig. 4. Original image (left) and the homogeneity values represented on a grey-level image (right).

- (b) the pixels adjacent to the seeds were inspected to check whether the value of the grey level was higher than the value T . The pixels with higher values were added to the nearest seed.
- (c) the pixels not lying adjacent to any seed were inspected in the same way. Those pixels with a grey-level value lower than the threshold T were considered as candidates to create a new seed. If these pixels formed a group larger than 32 pixels, the group was considered as a new seed. This step represented a modification of the original algorithm, adapted to detect defects that, because of their small size, could not form a representative homogeneous colour region in the entire image at the beginning of the process.

The iteration process stopped when all of the pixels in the image were assigned to a seed.

3.1.4. Region merging

After the region-growing process, the image appeared over-segmented into more regions than the actual objects of interest. To correct this situation, the next step consisted in joining regions with similar features. Similar objects had similar colours. Following this reasoning, the criterion for joining the regions was based on colour similarity and adjacency. Thus, adjacent regions with similar colours were joined to form a single region. The first step consisted in calculating the average colour of the pixels of each segmented region in the HSI colour space, this information being extracted from the original image of 2^{24} colours. The colour coordinates were converted from the original RGB colour space using the equations described in Poynton (1997). The Euclidean distances between the average colour of each region was used to join them, in such a way that if the distance between two adjacent regions was lower than a specific threshold, they were merged. An estimation of the colour difference, ΔE , between two regions was estimated using the Eq. (2).

$$\Delta E = \sqrt{\Delta V_1^2 + \Delta V_2^2 + \Delta V_3^2} \quad (2)$$

where V_1 , V_2 , V_3 correspond to the HSI colour coordinates, respectively, normalised between [0..1].

Typically, this technique is based on the aggregation method (Duda & Hart, 1973), which describes an iterative process where the distance among all of the adjacent regions is calculated. Then, only the pair with the lowest distance is merged and the distances are recalculated again for a new iteration. This process is repeated until the lowest distance is greater than a threshold. In our approach, every pair of adjacent regions whose Euclidean colour distance was lower than the threshold were merged in each iteration, which required fewer iterations to achieve convergence than the classical approach.

At the end of the process of region merging, the image was segmented in different unlabeled regions. At this point, the system did not have information about what object

class was represented by each region. The area of the sound skin is generally much larger than the area of any individual defect. For this reason, the largest of the segmented

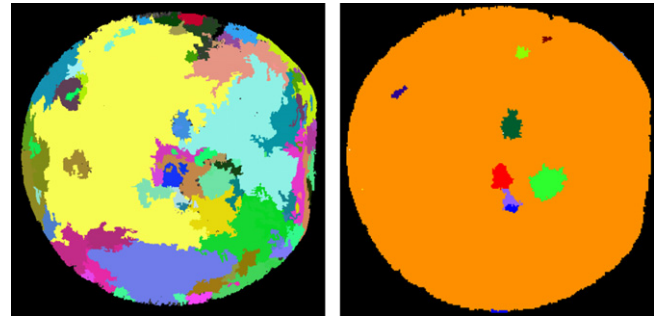


Fig. 5. Result after the region-growing process (left) and the region merging process (right).

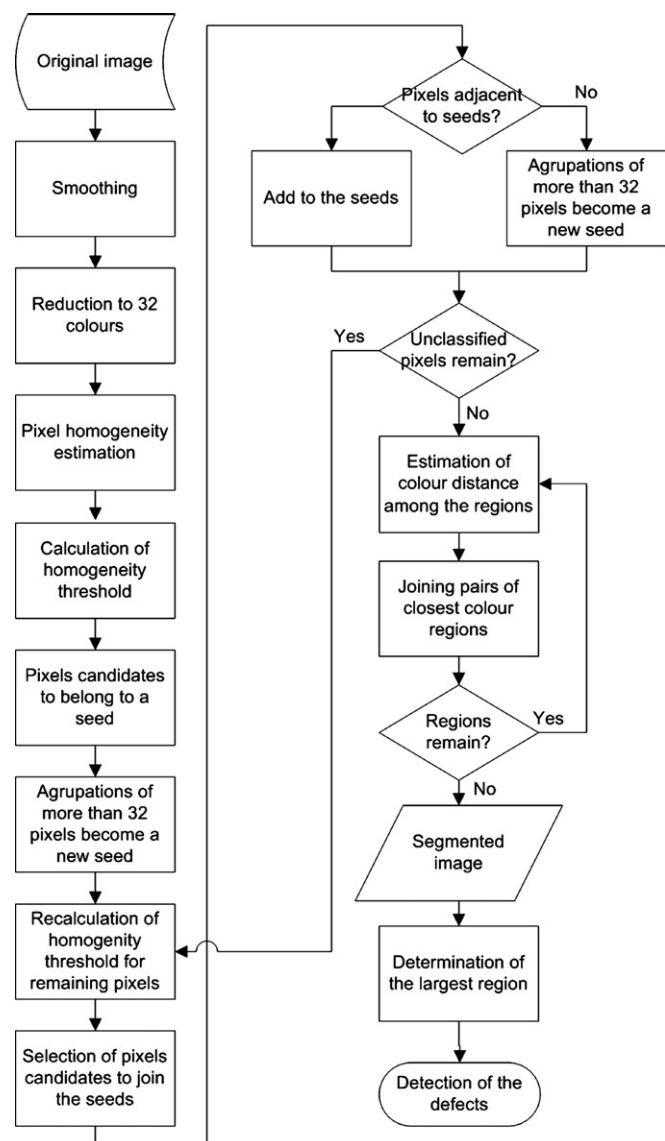


Fig. 6. Flowchart of the unsupervised defect detection algorithm that was developed.

regions was assumed to correspond to the sound skin and the rest were considered to be defects. This approach would have failed if the area of any individual defect had been bigger than that of the sound peel. However, the tests performed demonstrated the suitability of the method. Fig. 5 shows the same fruit, just after the region-growing iteration process and after the region merging. The sound skin and the defects, represented by the small regions, are clearly visible. The flowchart of the whole algorithm, from the original image to the detection of the defects is shown in Fig. 6.

3.1.5. Performance of the algorithm

All of the images were processed using the algorithm described here with no modifications or particular adjustments for the different varieties. To compare the results obtained by the system with the actual damage, the images were labelled and the number of individual defects present in each was noted. The result of the algorithm was a file containing the number of individual defects for each image. The evaluation of the ability of the unsupervised vision system to detect defects in citrus fruits was carried out by an expert who compared the automatic segmentation of the images with the visual appreciation of each fruit, in order to check whether all the damages had been correctly detected by the vision system.

4. Results and discussion

The main result of this work is the development of a new region-oriented image segmentation algorithm, designed for detecting external defects in citrus fruits. The algorithm is robust against the natural colour variation of different varieties and species of citrus fruits without previous training or adjustments during the tests.

Table 2 shows the result of defect detection for the different varieties used in the experiments. The ‘Detected’ row shows the defects that the system was able to detect and the cases where no defects were found in fruits that did not contain any defects. ‘Not detected’ were the defects that the expert found in the fruit but which were not detected by the vision system. Sound skin areas mistakenly identified as defects by the system are shown in the table as ‘False detections’. The percentage of false detections was calculated over the total number of detections, which was the sum of the correctly detected defects and the false detections. There are no great differences in the detection of the defects as far as the variety is concerned. Since the hue of the fruits is different for each variety, the algorithm

can be considered as robust against the natural colour variations of the varieties that were studied, which demonstrated the feasibility of the algorithm for inspecting different species of citrus fruits without adjustments. The success rate was slightly lower in oranges than in mandarins, probably due to the greater diameter of the oranges, which increased the error in the border areas of the fruits.

The distribution of the detections according to the type of each defect is shown in Table 3. Most of the undetected defects correspond to scale (15.5%), thrips scarring (6.2%) and oleocellosis (6.6%). Due to the small size of scale, the affected areas were not considered as seeds by the segmentation algorithm and therefore, they were mistakenly taken to be sound skin. The cases of thrips scarring and oleocellosis are different: what happened here is that the colour of these damages was sometimes close to that of the sound skin, and so the algorithm failed to differentiate between them.

The different parts of the new algorithm, such as smoothing, colour reduction or region-growing, are based on existing algorithms that were modified to adapt them to the problem of the detection of the different kind of defects that citrus fruits can present. The objective of this method is to detect the defects, not to identify them. In this sense, it is significant that no modifications, adaptations or human interventions were needed to inspect all the citrus fruits of different varieties and even different species harvested in different periods of the season.

The stem and several types of damage, including all of the most dangerous defects (anthracnose, stem-end injury, medfly and green mould), were correctly detected in 100% of cases and the average rate of correctly detected defects

Table 3
Results of the detection system according to the type of each defect

Damages	Number of defects	Detections (%)
Medfly	41	100.0
Sooty mould	72	100.0
Thrips scarring	736	93.8
Scarring	250	98.8
Oleocellosis	99	93.4
Scale	393	84.5
Green mould	57	100.0
Phytotoxicity	213	100.0
Chilling injury	178	97.8
Stem-end injury	39	100.0
Anthracnose	54	100.0
Stem	162	100.0

Table 2
Defect detection results of the unsupervised segmentation algorithm, depending on the variety

Defects	Variety					
	Navelina (%)	Valencia (%)	Marisol (%)	Clemenules (%)	Fortune (%)	Total (%)
Detected	94.6	91.3	94.2	96.6	95.3	94.2
Not detected	5.4	8.7	5.8	3.4	4.7	5.8
False detections	3.1	7.6	3.3	4.4	1.8	4.0

was 94% – both of which can be considered to be good results. In general, there was a low percentage of false detections, most of them located on the border of the fruits. Thus, most of the false detections could probably be avoided by simply not inspecting the borders of the fruit in the images. Not inspecting the borders, however, does not imply losing efficacy, since in the on-line automatic computer vision systems for fruit inspection, the fruits rotate, thus allowing the system to inspect most of the fruit surfaces by acquiring different images while they pass below the camera.

Although this work is focused on citrus fruits, the algorithm developed has been tested successfully in different species of citrus, as mandarins and oranges, with different colours and sizes. Probably, it could also work properly in other fruits having a single skin colour affected by similar type of defects, as some varieties of peaches or apples. However, it would be important to have in account the particularities of each of fruit, as the presence of shape irregularities in the stem area or large stems.

The segmentation algorithm proposed here does not distinguish between the stem and the defects. Identifying the type of each defect or the stem can be performed in later processes, but was not an objective of this work.

5. Conclusions

A new region-oriented image segmentation algorithm, based on unsupervised techniques, has been proposed for detecting the external defects of citrus fruits. The algorithm is robust against different varieties and species of citrus fruit and does not need previous manual training or adjustments to adapt the system to work with different batches of fruit or changes in the lighting conditions.

The generation of new seeds during all the iterative region-growing process differentiates this method from the classical region-growing segmentation techniques, allowing the segmentation of the smallest defects of citrus skin.

The algorithm was tested using the images of 2294 defects and stems in different varieties and species of citrus fruits. Assuming that the largest region of interest corresponds to the sound peel, the algorithm succeeded in segmenting correctly 94% of the defects and stems present in the images, without the introduction of changes in the configuration parameters.

Acknowledgements

This work was partially funded by the Spanish Ministry of Science and Technology (MCYT) by means of the Plan Nacional de Investigación Científica, Desarrollo e Innovación Tecnológica (I+D+I) and European FEDER funds, through Project DPI-2003-09173-C02-02 “Técnicas avanzadas de visión por computador para el reconocimiento e identificación automática de los defectos externos de los cítricos”.

References

- Albiol, A., Torres, L., & Delp, E. J. (2001). An unsupervised color image segmentation algorithm for face detection applications. In *Proceedings of the 2001 international conference on image processing* (pp. 681–684). Thessaloniki, Greece.
- Aleixos, N., Blasco, J., Navarrón, F., & Moltó, E. (2002). Multispectral inspection of citrus in real-time using machine vision and digital signal processors. *Computers and Electronics in Agriculture*, 33(2), 121–137.
- Aleixos, N., Blasco, J., & Moltó, E. (1999). Design of a vision system for real-time inspection of oranges. In *VIII national symposium on pattern recognition and image analysis* (pp. 387–394). Bilbao, Spain.
- Bhalerao, A., & Wilson, R. (2001). Unsupervised image segmentation combining region and boundary estimation. *Image and vision computing*, 19(6), 353–386.
- Blasco, J., Aleixos, N., & Moltó, E. (2003). Machine vision system for automatic quality grading of fruit. *Biosystems Engineering*, 85(4), 415–423.
- Brodie, J. R., Hansen, A. C., & Reid, J. F. (1994). Size assessment of stacked logs via the Hough Transform. *Transactions of the ASAE*, 37(1), 303–310.
- Brox, T., Rousson, M., Deriche, R., & Weickert, J. (2003). Unsupervised segmentation incorporating colour, texture and motion. *Lecture Notes in Computer Science*, 2756, 353–360.
- Chadda, N., Tan, W. C., & Meng, T. H. Y. (1994). Color quantization of images based on human vision perception. In *Proceedings of the international conference on acoustics, speech, and signal processing, ICASSP* (pp. 89–92). Adelaide, Australia.
- Deng, Y., Manjunath, B. S., & Shin, H. (1999). Color image segmentation. In *Proceedings of the IEEE Computer Society Conference on Computer Vision and Pattern Recognition (CVPR)* (pp. 446–451). CO, USA: Ft. Collins.
- Díaz, R., Faus, G., Blasco, M., Blasco, J., & Moltó, E. (2000). The application of a fast algorithm for the classification of olives by machine vision. *Food Research International*, 33, 305–309.
- Díaz, R., Gil, L., Serrano, C., Blasco, M., Moltó, E., & Blasco, J. (2004). Comparison of three algorithms in the classification of table olives by means of computer vision. *Journal of Food Engineering*, 61(1), 101–107.
- Du, C. J., & Sun, D. W. (2005). Pizza sauce spread classification using colour vision and support vector machines. *Journal of Food Engineering*, 66(2), 137–145.
- Duda, R. O., & Hart, P. E. (1973). *Pattern classification and scene analysis*. New York: John Wiley & Sons Inc..
- Fu, K. S., & Mui, J. K. (1981). A survey on image segmentation. *Pattern Recognition*, 13, 3–16.
- Gonzalez, R. C., & Woods, R. E. (2002). *Digital image processing*. NJ, USA: Prentice Hall.
- Hahn, F. (2002). Multi-spectral prediction of unripe tomatoes. *Biosystems Engineering*, 81(2), 147–155.
- Hofmann, T., & Buhmann, J. M. (1998). Competitive learning algorithms for robust vector quantization. *IEEE Transactions on Signal Processing*, 46(6), 1665–1675.
- Jing, F., Li, M., Zhang, H. J., & Zhang, B. (2003). Unsupervised image segmentation using local homogeneity analysis. In *Proceedings of IEEE international symposium on circuits and systems* (pp. 456–459). Bangkok, Thailand.
- Kenney, C., Deng, Y., Manjunath, B. S., & Hewer, G. (2001). Peer group image enhancement. *IEEE Transactions on Image Processing*, 10, 326–334.
- Kiliç, K., Hakki-Boyaci, I., Köksel, H., & Küsmenoğlu, I. (2007). A classification system for beans using computer vision system and artificial neural networks. *Journal of Food Engineering*, 78(3), 897–904.
- Leemans, V., & Destain, M. F. (2004). A real-time grading method of apples based on features extracted from defects. *Journal of Food Engineering*, 61(1), 83–89.

- Lloyd, S. P. (1982). Least squares quantization in PCM. *IEEE Transactions on Information Theory*, 28, 127–135.
- Lucchese, L., & Mitra, S. K. (1999). Unsupervised low-frequency driven segmentation of color images. In *Proceedings of the 1999 IEEE international conference on image processing* (pp. 240–244). Kobe, Japan.
- Marchant, J. A., & Onyango, C. M. (2003). Comparison of a Bayesian classifier with a multilayer feed-forward neural network using the example of plant/weed/soil discrimination. *Computers and Electronics in Agriculture*, 39(1), 3–22.
- Martínez-Usó, A., Pla, F., & García, P. (2003). A quadtree-based unsupervised segmentation algorithm for fruit visual inspection. In *first Iberian conference on pattern recognition and image analysis* (pp. 510–517). Mallorca, Spain.
- Meuleman, J., & Van Kaam, C. (2001). Unsupervised image segmentation with neural networks. *Acta Horticulturae (ISHS)*, 562, 101–108.
- Moltó, E., Aleixos, N., Blasco, J., & Navarrón, F. (2000). Low-cost, real-time inspection of oranges using machine vision, In *International conference on modelling and control in agriculture, horticulture and post-harvested processing, agricontrol 2000* (pp. 309–314). Wageningen, The Netherlands.
- Moshou, D., Bravo, C., West, J., McCartney, A., & Ramon, H. (2004). Automatic detection of ‘yellow rust’ in wheat using reflectance measurements and neural networks. *Computers and Electronics in Agriculture*, 44(3), 173–188.
- Noordam, J. C., Van Den Broek, W. H. A. M., & Buydens, L. M. C. (2003). Unsupervised segmentation of predefined shapes in multivariate images. *Journal of Chemometrics*, 17, 274–282.
- Poynton, C. (1997). Frequently-asked questions about color. Available on-line at <http://www.poynton.com/PDFs/ColorFAQ.pdf>. [Last accessed January 2007.]
- Steinmetz, V., Roger, J. M., Moltó, E., & Blasco, J. (1999). On-line fusion of colour camera and spectrophotometer for sugar content prediction of apples. *Journal of Agricultural Engineering Research*, 73, 207–216.
- Sun, D. W., & Du, C. J. (2004). Segmentation of complex food images by stick growing and merging algorithm. *Journal of Food Engineering*, 61(1), 17–26.
- Unay, D., & Gosselin, B. (2007). Stem and calyx recognition on ‘Jonagold’ apples by pattern recognition. *Journal of Food Engineering*, 78(2), 597–605.